CDF/PHYS/EXO/PUBLIC/10930

Search for a Higgs boson multiplet in $p\bar{p}$ collisions at $\sqrt{s} = 1.96$ TeV

Abstract

We present a search for a Higgs sector which includes a heavy Higgs (H_0), a charged Higgs (h^+) and a light higgs h_0, with decays leading to a $W^{\pm}W^{\mp}b\bar{b}$ final state. We use events with exactly one lepton, missing transverse energy and at least four jets in data with integrated luminosity of 8.7 fb^{-1}. We find the data to be consistent with the Standard Model and set cross-section upper limits as a function of H_0 and h^+ masses.

PACS numbers: 12.60.-i, 13.85.Rm, 14.80.-j

The study of the mechanism of electroweak symmetry breaking is one of the major thrusts of the experimental high energy physics program. Following the discovery of a Higgs-like boson at ATLAS [1] and CMS [2] near 126 GeV/c^2, the most pressing question is whether this state is in fact the Higgs boson of the minimal standard model, part of an extended Higgs sector (such as that of the minimal supersymmetric standard model, or MSSM [3]), a composite Higgs [4], or a completely different particle with Higgs-like couplings (such as a radion in warped extra dimensions [5] or dilaton [6]).

In this paper, we search for an extended Higgs sector which includes a light neutral Higgs boson at 126 GeV/c^2. Rather than assume a particular theoretical framework (such as the MSSM), we take a phenomenological approach, using a general 2-Higgs doublet model as a convenient simplified model [7] to parameterize the signals. This approach motivates a variety of signals with final states involving the heaviest standard model particles which have the strongest couplings to the Higgs sector [8, 9]. The WW final state is enhanced by WW scattering in models where the Higgs sector is strongly coupled [10], and this signal has been the subject of much detailed investigation [11]. The phenomenology of resonant production of the final states Zh^0 [12] and W^+W^-Z [13] have also been investigated.

In this paper, we focus on the final state $W^+W^-b\bar{b}$ [14], which can have a large production rate from the process $gg \to H^0$ followed by $H^0 \to H^\pm W^\mp$ with $H^+ \to W^+h^0 \to W^+b\bar{b}$. The $WWbb$ final state is the decay mode of top-quark pair production, and has been extensively studied. However, though searches have been performed for charged Higgs decays $t \to H^+b$ [15], there has been no previous search for Higgs resonances as described here. An alternative decay mode, $H^+ \to t\bar{b} \to W^+b\bar{b}$, is left to future studies.

We analyze a sample of events corresponding to an integrated luminosity of 8.7±0.5 fb^{-1} recorded by the CDF II detector [16], a general purpose detector designed to study $p\overline{p}$ collisions at $\sqrt{s} = 1.96$ TeV produced by the Fermilab Tevatron collider. CDF's tracking system consists of a silicon microstrip tracker and a drift chamber that are immersed in a 1.4 T axial magnetic field [17]. Electromagnetic and hadronic calorimeters surrounding the tracking system measure particle energies, with muon detection provided by an additional system of drift chambers located outside the calorimeters.

Events are selected online (triggered) by the requirement of an e or μ candidate [18] with transverse momentum p_T [19] greater than 18 GeV/c. After trigger selection, events are retained if the electron or muon candidate has a pseudorapidity $|\eta| < 1.1$ [19], $p_T > 20$

GeV/c and satisfies the standard CDF identification and isolation requirements [18]. We reconstruct jets in the calorimeter using the JETCLU [20] algorithm with a clustering radius of 0.4 in $\eta-\phi$ space, and calibrated using the techniques outlined in Ref. [21]. Jets are required to have transverse energy $E_T > 15$ GeV and $|\eta| < 2.4$. Missing transverse momentum [22] is reconstructed using calorimeter and muon information [18]; in this experimental signature the missing transverse momentum is mostly due to the neutrino from the leptonically decaying W boson.

The signature of $H^0 \to W^- H^+ \to W^- W^+ h^0 \to W^- W^+ b\bar{b}$ is a charged lepton (e or μ), missing transverse momentum, two jets arising from b quarks, and two additional jets from the W-boson hadronic decay. We select events with exactly one electron or muon, at least four jets, and missing transverse momentum greater than 20 GeV/c. Since such a signal would have two jets originating from b quarks, we require (with minimal loss of efficiency) evidence of decay of a b hadron in at least one jet. This requirement, called b-tagging, makes use of the SECVTX algorithm which identifies jets from b quarks via their secondary vertices [23].

We model the production of H^0 with m_{H^0} = 325-1100 GeV/c^2 and subsequent decays $H^0 \to W h^+$ with $m_{h^+} = 225 - 600$ GeV/c^2 and decays $h^+ \to W^+ h$ with $m_h = 126$ GeV/c^2, all with MADGRAPH [24]. Additional radiation, hadronization and showering are described by PYTHIA [25]. The detector response for all simulated samples is modeled by the GEANT-based CDF II detector simulation [26].

The dominant SM background to the $t\bar{t}$ signature is top-quark pair production. We model this background using PYTHIA $t\bar{t}$ production with a top-quark mass $m_t = 172.5$ GeV/c^2 [27]. We normalize the $t\bar{t}$ background to the theoretical calculation at next-to-next-to-leading order (NNLO) in α_s [28]. In addition, events generated by a next-to-leading order generator, MC@NLO [29] are used in estimating an uncertainty in modeling the radiation of an additional jet.

The second largest SM background process is the associated production of a W boson and jets. Samples of W-boson+jets events with light- and heavy-flavor (b, c) quark jets are generated using ALPGEN [30], and interfaced with a parton-shower model from PYTHIA. The W-boson+jets samples are normalized to the measured W-boson production cross section, with an additional multiplicative factor for the relative contribution of heavy- and light-flavor jets, following the same technique utilized previously in measuring the top-quark pair-production cross section [23].

Backgrounds due to production of a Z boson with additional jets, where the second lepton from the Z-boson decay is not reconstructed, are small compared to the W-boson background and are modeled using events generated with ALPGEN, and interfaced with the parton-shower model from PYTHIA. The multi-jet background, in which a jet is misreconstructed as a lepton, is modeled using events triggered on jets normalized to a background-dominated region at low missing transverse momentum where the multi-jet background is large.

The SM backgrounds due to single top quark and diboson production are modeled using MADGRAPH interfaced with PYTHIA parton-shower models and PYTHIA, respectively, and normalized to next-to-leading-order cross sections [31, 32].

The resonant mass reconstruction is started by first considering the leptonic W. The missing transverse energy per event is assumed to be the transverse momentum of the neutrino resulting from the leptonic W decay. This neutrino is then paired with the exactly one lepton per event as the decay products of the W, with neutrino psuedorapidity taken to be the lowest value that yields W mass closest to 80.4 GeV. The reconstruction strategy for the hadronically decaying W is to take combinations of the at least four jets, avoiding b-tagged jets when possible, and labelling the two whose reconstructed mass is closest to 80.4 GeV as decay products. In the event of only one or zero non-b-tagged jets, the same process is used, only b-tagged jets are now considered as candidates as well. The light neutral Higgs is reconstructed from the remaining b-tagged jets. In the event of only one or zero, as in the high $b\bar{b}WW$ mass 0 b-tagged jets control region to be described momentarily, the jet(s) with highest transverse momentum not associated with the hadronic W decay are used instead. Figure 1 shows distributions of the reconstructed mass for several choices of Higgs masses.

We enhance the signal-to-background ratio by making requirements on the mass of the $WWbb$ and Wbb systems, and search for a signal as an excess of events above expectations from backgrounds in event distributions versus the mass of the $b\bar{b}$ system ($h \to b\bar{b}$). Backgrounds, in which no resonance is present, have broad, smoothly decreasing distributions while a signal would be reconstructed near the resonance mass.

We consider several sources of systematic uncertainty on the predicted background rates and distributions, as well as on the expectations for a signal. Each systematic uncertainty affects the expected sensitivity to a signal, expressed as an expected cross-section upper limit in the no-signal assumption. The dominant systematic uncertainty is the jet energy

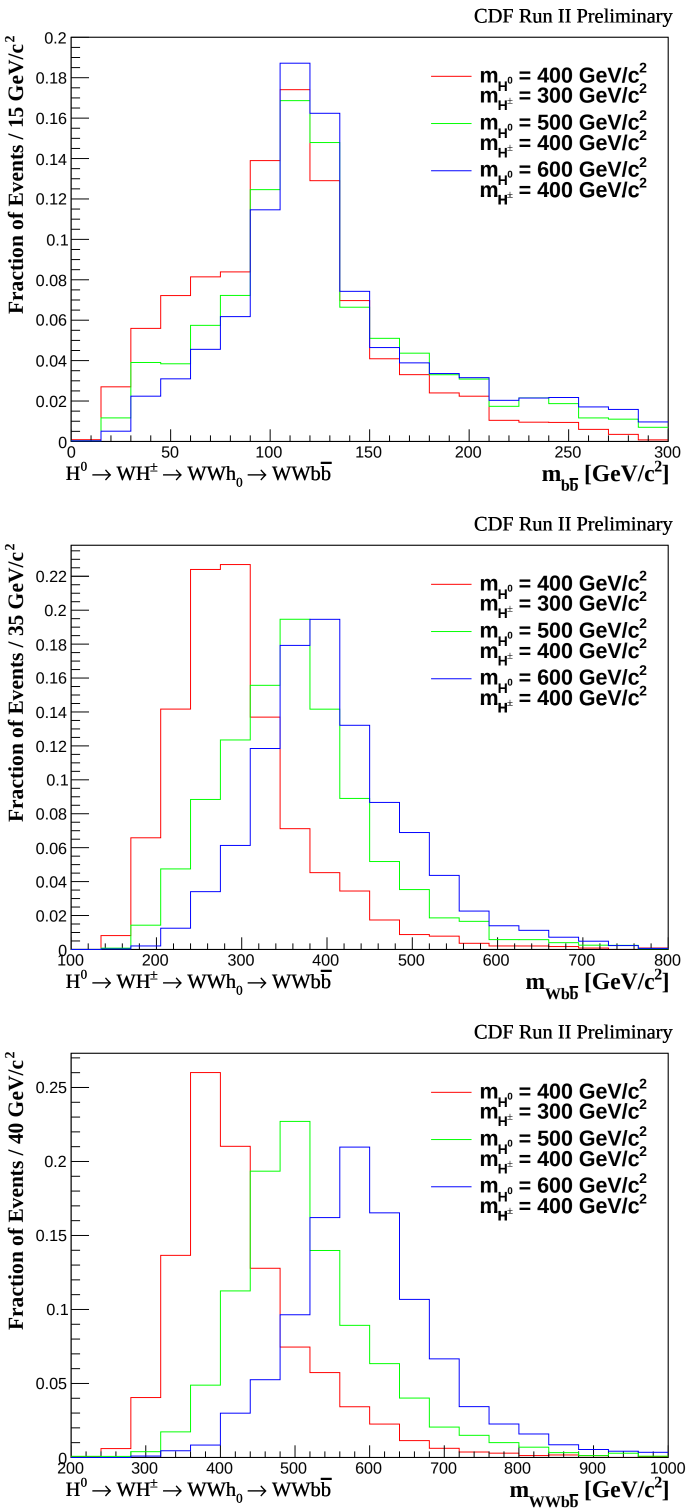

FIG. 1: Distribution of reconstructed Higgs mass in simulated events.

scale (JES) uncertainty [21], followed by theoretical uncertainties on the cross sections of the background processes. To probe the description of the additional jet, we compare our nominal $t\bar{t}$ model to one generated by MC@NLO and take the full difference as a systematic uncertainty. We also consider systematic uncertainties associated with the description of initial- and final-state radiation [33], uncertainties in the efficiency of reconstructing leptons and identifying b-quark jets, and uncertainties in the contribution from multiple proton interactions. In addition, we consider a variation of the Q^2 scale of W-boson+jet events in ALGPEN. In each case, we treat the unknown underlying quantity as a nuisance parameter and measure the distortion of the $m_{b\bar{b}}$ spectrum for positive and negative fluctuations of the underlying quantity. Table I lists the contributions of each of these sources of systematic uncertainty to the yields.

TABLE I: Contributions to the systematic uncertainty on the expected numbers of events for the two main background processes, the total background yield, and an example 500 GeV/c^2 resonance signal with an assumed total cross section of 1 pb.

				$H^0 \to WH^\pm \to WWh_0 \to WWb\bar{b}$
Process	$t\bar{t}$	W-boson+jets	Total Bg.	Higgs
Yield	229	43	294	341
JES	23%	-	17%	12%
Radiation	3%	-	2%	8%
Q^2 scale	-	18%	3%	-
Nvtx	1%	6%	2%	-
$t\bar{t}$ generator	5%	-	4%	-
Normalization	10%	30%	16%	-
Total syst. uncert.	26%	35%	24%	15%

We validate our modeling of the SM backgrounds in four background-dominated control regions. Each control region continues to have the one lepton and at least four jet requirements with additional restrictions per region. The first control region models low $b\bar{b}$ mass reconstructions, with restrictions at least one b-tagged jet and $b\bar{b}$ mass less than 100 GeV. The second region models low $b\bar{b}W$ mass reconstruction, with restrictions at least one b-tagged jet and $b\bar{b}W$ mass less than 250 GeV. The third region models low $b\bar{b}WW$

mass reconstruction, with restrictions at least one b-tagged jet and $b\bar{b}WW$ mass less than 450 GeV. The fourth and last region models high $b\bar{b}WW$ mass reconstruction, with requirements $b\bar{b}WW$ mass greater than 450 GeV and exactly 0 b-tagged jets. As shown in Fig. 2, the backgrounds are well modeled within systematic uncertainties.

Figure 3 shows the observed distribution of events in the signal region compared to possible signals and estimated backgrounds. At each Higgs mass hypothesis, we fit the most likely value of the Higgs cross section by performing a binned maximum-likelihood fit in the $m_{b\bar{b}}$ variable, allowing for systematic and statistical fluctuations via template morphing [34]. No evidence is found for the presence of Higgs resonance in $WWb\bar{b}$ events, so we set upper limits on Higgs production at 95% confidence level using the CLs method [35], without profiling the systematic uncertainties. The observed limits are consistent with expectation for the background-only hypothesis. See Fig. 4 and Table II.

In conclusion, we report on the first search for multiple Higgs bosons in cascades decays. For each accepted event, we reconstruct the resonance mass ($m_{b\bar{b}}$), and find the data to be consistent with SM background predictions. We calculate 95% CL upper limits on the cross section of such resonance production from 1.3 pb to 0.015 pb for masses ranging from ($m_{H^0} = 325, m_{h^+} = 225$) GeV/$c^2$ to ($m_{H^0} = 1100, m_{h^+} = 600$) GeV/$c^2$ respectively and interpret the limits in terms of a simplified two-higgs doublet model.

We thank the Fermilab staff and the technical staffs of the participating institutions for their vital contributions. This work was supported by the U.S. Department of Energy and National Science Foundation; the Italian Istituto Nazionale di Fisica Nucleare; the Ministry of Education, Culture, Sports, Science and Technology of Japan; the Natural Sciences and Engineering Research Council of Canada; the National Science Council of the Republic of China; the Swiss National Science Foundation; the A.P. Sloan Foundation; the Bundesministerium für Bildung und Forschung, Germany; the Korean World Class University Program, the National Research Foundation of Korea; the Science and Technology Facilities Council and the Royal Society, UK; the Russian Foundation for Basic Research; the Ministerio de Ciencia e Innovación, and Programa Consolider-Ingenio 2010, Spain; the Slovak R&D Agency; the Academy of Finland; and the Australian Research Council (ARC).

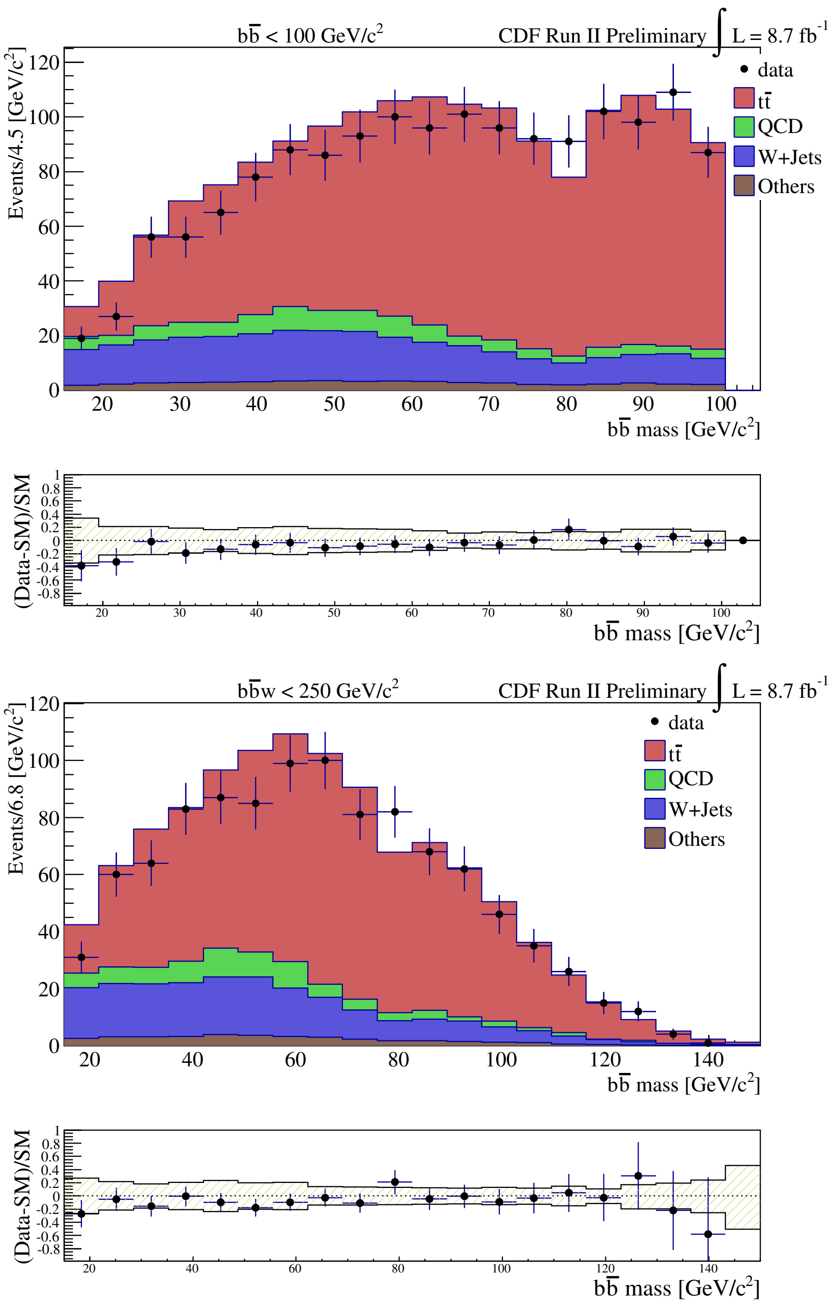

FIG. 2: Distribution of events versus reconstructed $b\bar{b}$ invariant mass ($m_{b\bar{b}}$) for observed data and expected backgrounds in two control regions. The lower panel give the relative difference between the observed and expected distributions; the hatched areas show the combined statistical and systematic uncertainties of the expected background. Top, low Wbb control region: events with at least four jets and $m_{Wbb} < 250$. Bottom, low $WWbb$ control region: events with at least four jets, exactly zero b-tags and $m_{WWbb} < 450$.

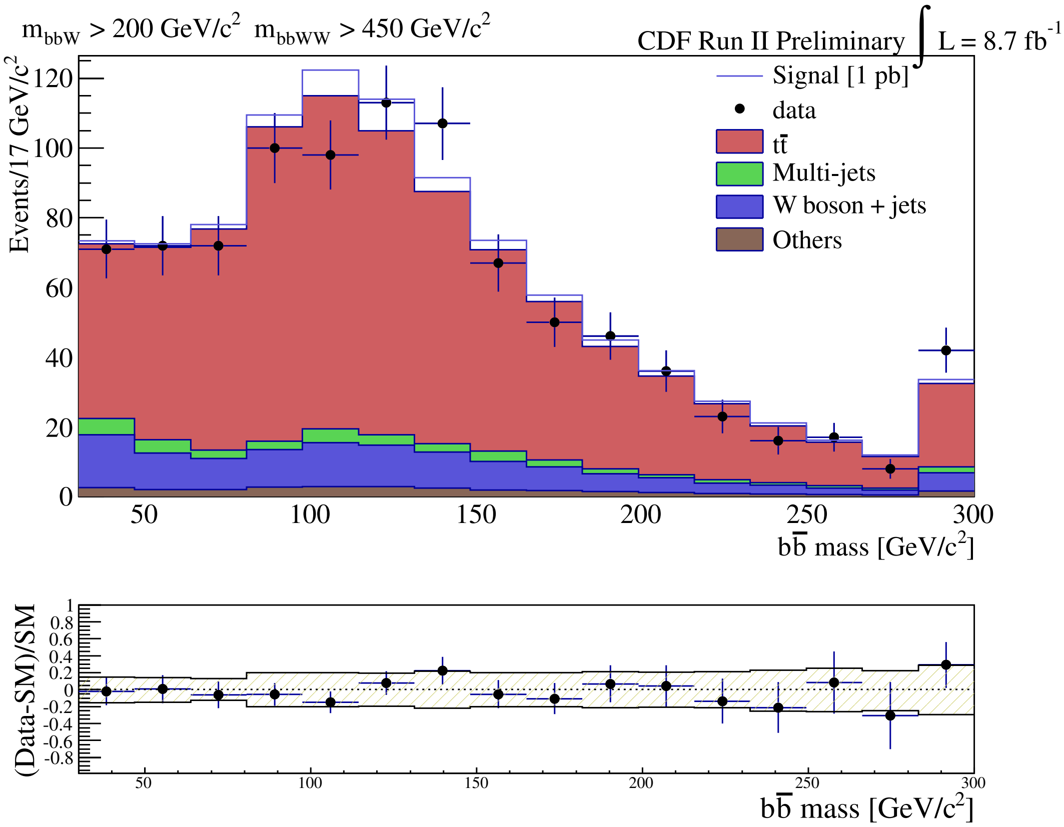

FIG. 3: Distribution of events versus reconstructed $b\bar{b}$ invariant mass ($m_{b\bar{b}}$), for observed data and expected backgrounds in the signal region. A signal hypotheses is shown, assuming a total cross section of 1 pb. The lower panel gives the relative difference between the observed and expected distributions; the hatched area shows the combined statistical and systematic uncertainties of the expected background.

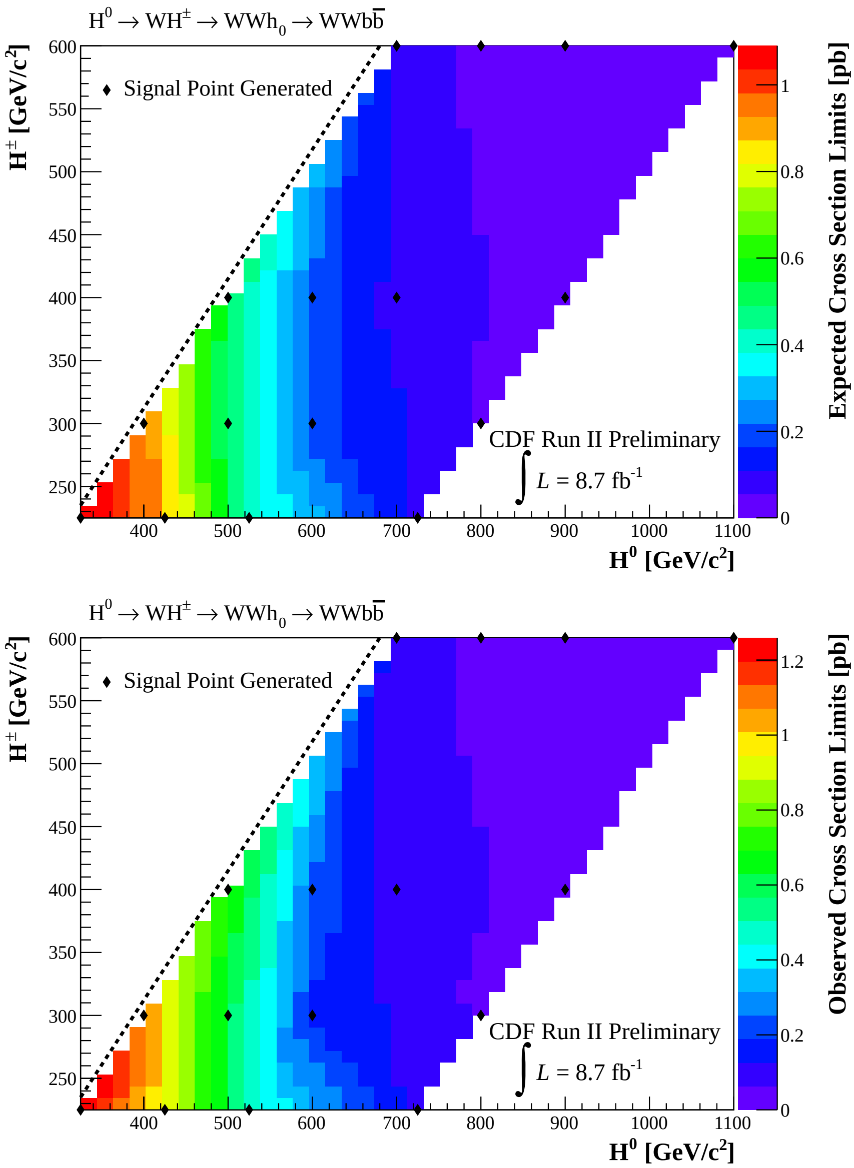

FIG. 4: Expected (top) and observed (bottom) upper limits at 95% CL on the cross-section as a function of the Higgs mass.

TABLE II: For each Higgs mass hypothesis, signal region cuts, the expected and observed limits at 95% CL on the production cross section times branching ratio, the theoretical prediction.

$H^0 \to WH^{\pm} \to WWh_0 \to WWb\bar{b}$

(m_{H^0}, m_{h^+}) (GeV)	m_{h^+} (GeV)	m_{H^0} (GeV)	Exp (Obs) Limit (pb)	Theory (pb)
325, 225	> 175	> 275	1.1 (1.3)	1.3
400, 300	> 225	> 325	0.96 (1.1)	1.1
425, 225	> 200	> 375	0.90 (0.96)	0.96
500, 300	> 200	> 450	0.47 (0.59)	0.60
500, 400	> 350	> 450	0.51 (0.70)	0.70
525, 225	> 100	> 500	0.42 (0.46)	0.46
600, 300	> 200	> 550	0.20 (0.18)	0.18
600, 400	> 350	> 550	0.21 (0.25)	0.25
700, 400	> 325	> 650	0.090 (0.10)	0.10
700, 600	> 450	> 650	0.10 (0.096)	0.10
725, 225	> 425	> 700	0.090 (0.12)	0.12
800, 300	> 275	> 750	0.050 (0.051)	0.051
800, 600	> 475	> 725	0.043 (0.046)	0.046
900, 400	> 450	> 775	0.028 (0.036)	0.036
900, 600	> 475	> 800	0.024 (0.029)	0.029
1100, 600	> 475	> 975	0.013 (0.015)	0.015

APPENDIX A: CONTROL REGION PLOTS

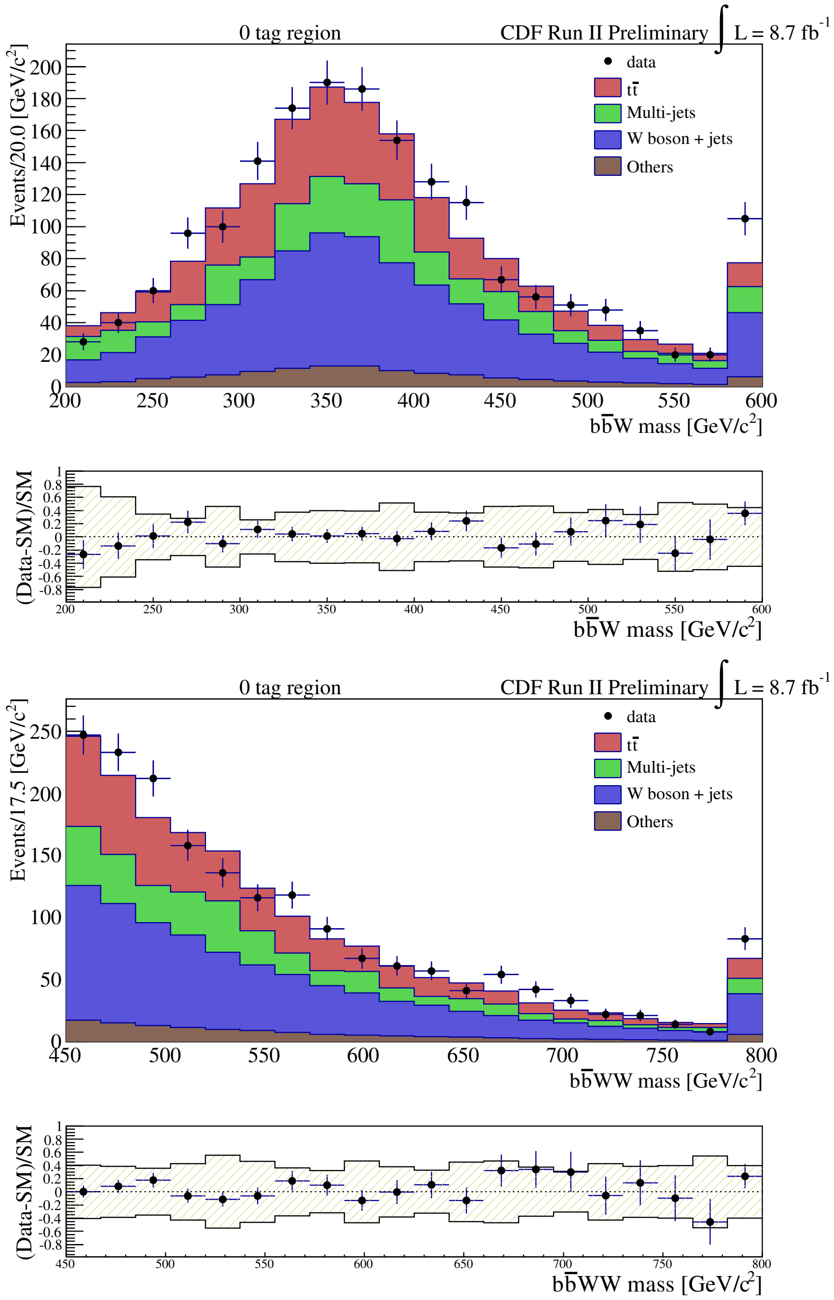

FIG. 5: Distribution of events versus reconstructed $b\bar{b}W$ invariant mass ($m_{b\bar{b}W}$) and $b\bar{b}WW$ invariant mass ($m_{b\bar{b}WW}$) for observed data and expected backgrounds in a control region with low $m_{b\bar{b}}$. The lower panel give the relative difference between the observed and expected distributions; the hatched areas show the combined statistical and systematic uncertainties of the expected background.

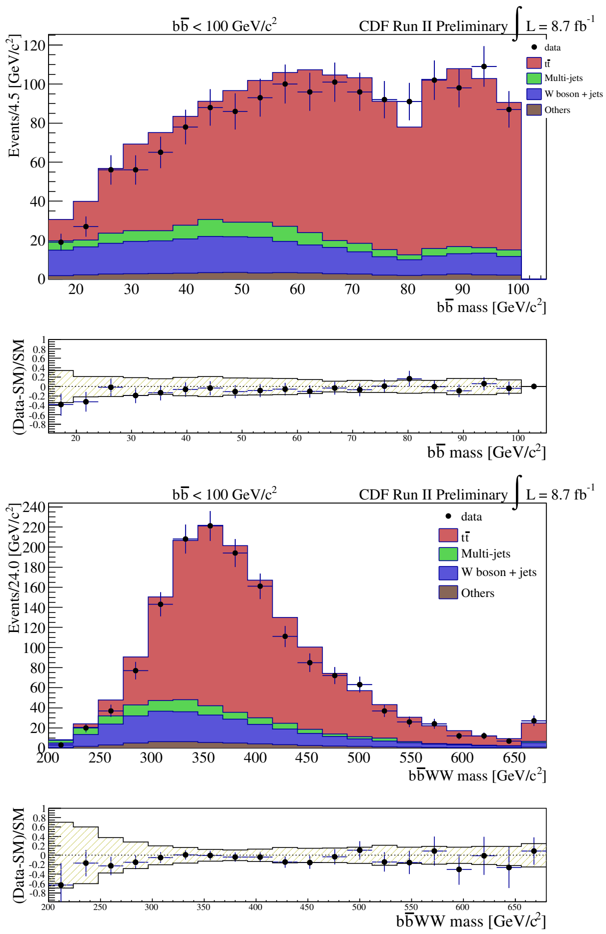

FIG. 6: Distribution of events versus reconstructed $b\bar{b}$ invariant mass ($m_{b\bar{b}}$) and $b\bar{b}WW$ invariant mass ($m_{b\bar{b}WW}$) for observed data and expected backgrounds in a control region with low $m_{b\bar{b}W}$. The lower panel give the relative difference between the observed and expected distributions; the hatched areas show the combined statistical and systematic uncertainties of the expected background.

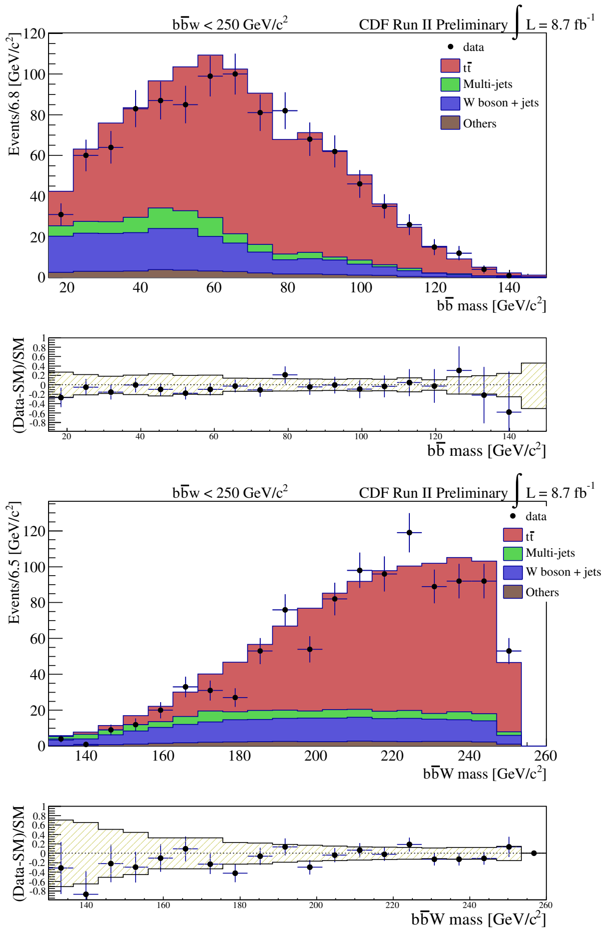

FIG. 7: Distribution of events versus reconstructed $b\bar{b}$ invariant mass ($m_{b\bar{b}}$) and $b\bar{b}W$ invariant mass ($m_{b\bar{b}W}$) for observed data and expected backgrounds in a control region with low $m_{b\bar{b}WW}$. The lower panel give the relative difference between the observed and expected distributions; the hatched areas show the combined statistical and systematic uncertainties of the expected background.

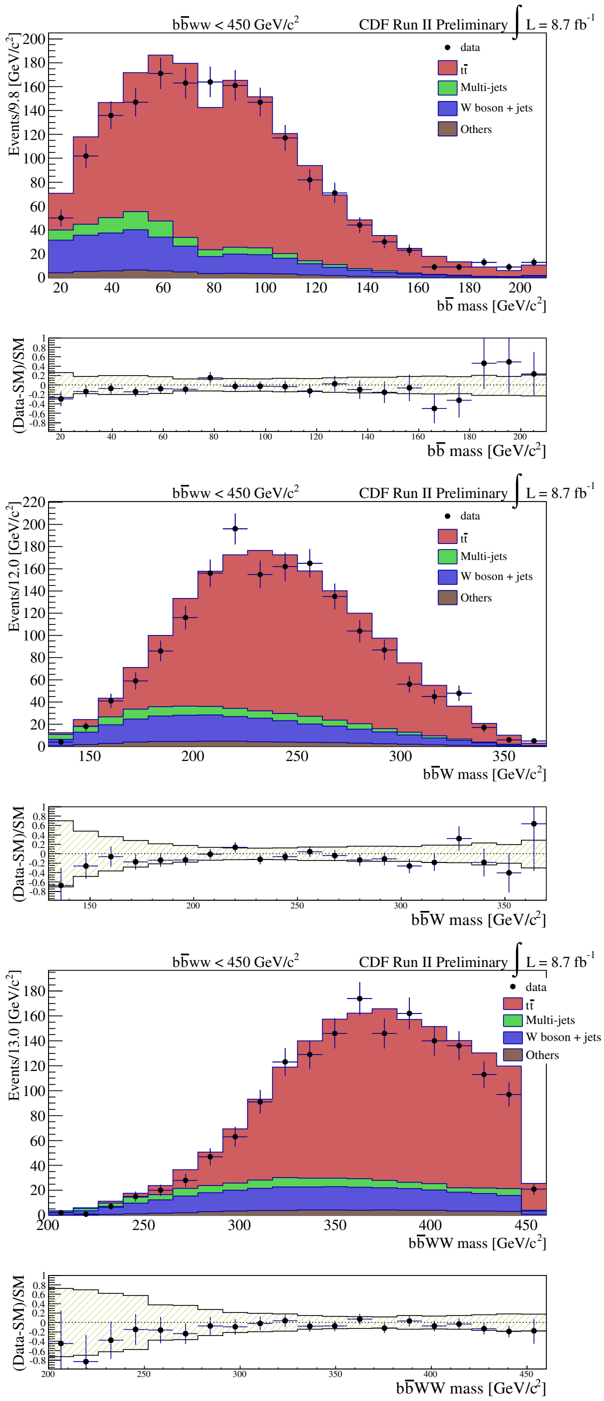

FIG. 8: Distribution of events versus reconstructed $b\bar{b}$ invariant mass ($m_{b\bar{b}}$),$b\bar{b}W$ invariant mass ($m_{b\bar{b}W}$), and $b\bar{b}WW$ invariant mass ($m_{b\bar{b}WW}$) for observed data and expected backgrounds in a control region with no b-tagged jets. The lower panel give the relative difference between the observed and expected distributions; the hatched areas show the combined statistical and systematic uncertainties of the expected background.

APPENDIX B: SIGNAL PLOTS

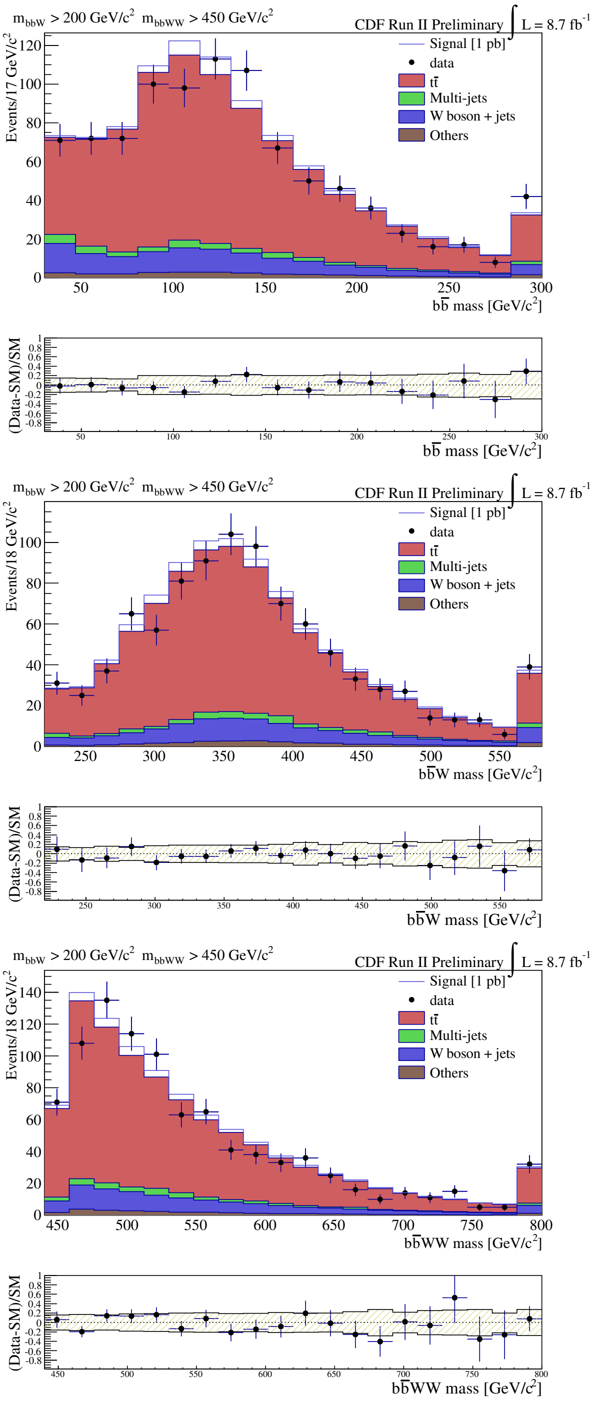

FIG. 9: Distribution of events versus reconstructed $b\bar{b}$ invariant mass ($m_{b\bar{b}}$) ,$b\bar{b}W$ invariant mass ($m_{b\bar{b}W}$), and $b\bar{b}WW$ invariant mass ($m_{b\bar{b}WW}$), for observed data and expected backgrounds in the signal region for $m_{H^0} = 500, m_{H^\pm} = 300$ GeV/c^2. A signal hypotheses is shown, assuming a total cross section of 1 pb. The lower panel gives the relative difference between the observed and expected distributions; the hatched area shows the combined statistical and systematic uncertainties of the expected background.

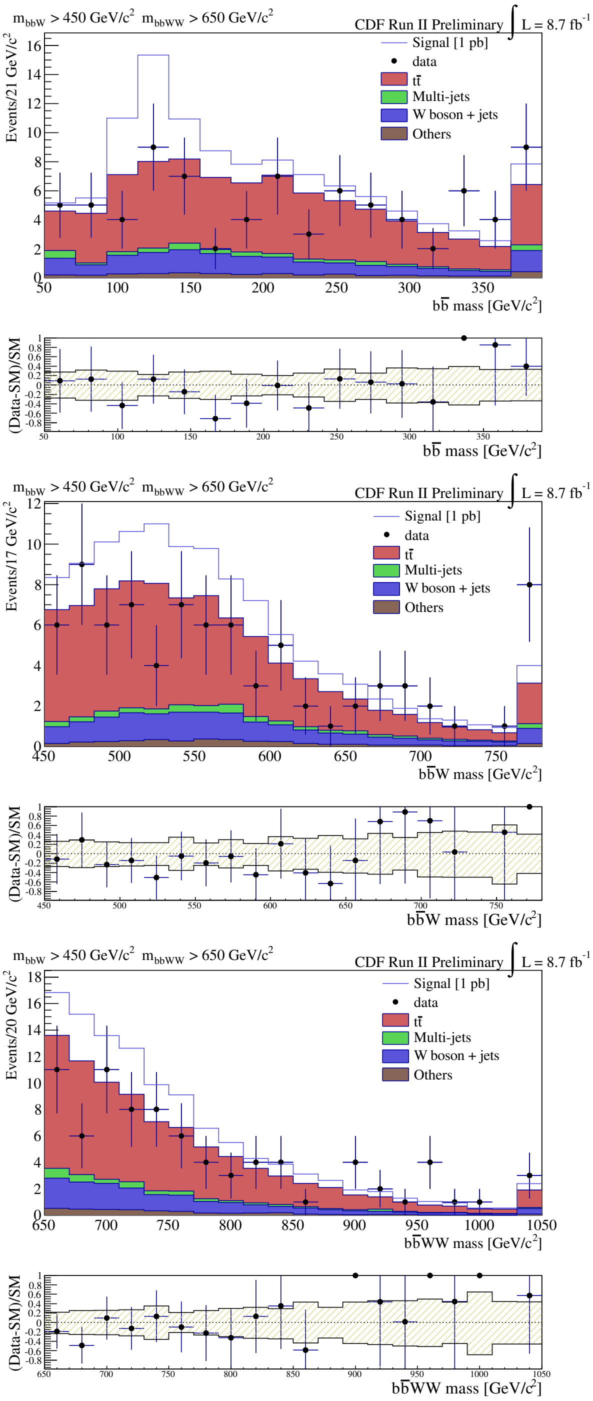

FIG. 10: Distribution of events versus reconstructed $b\bar{b}$ invariant mass ($m_{b\bar{b}}$) ,$b\bar{b}W$ invariant mass ($m_{b\bar{b}W}$), and $b\bar{b}WW$ invariant mass ($m_{b\bar{b}WW}$), for observed data and expected backgrounds in the signal region for $m_{H^0} = 700, m_{H^\pm} = 600$ GeV/c^2. A signal hypotheses is shown, assuming a total cross section of 1 pb. The lower panel gives the relative difference between the observed and expected distributions; the hatched area shows the combined statistical and systematic uncertainties of the expected background.

[1] G. Aad *et al.* [ATLAS Collaboration], Phys. Lett. B **716**, 1 (2012).

[2] S. Chatrchyan *et al.* [CMS Collaboration], Phys. Lett. B **716**, 30 (2012).

[3] H. P. Nilles, Phys. Rept. **110** 1-162 (1984); H. E. Haber and G. L. Kane, Phys. Rept. **117** 75-263 (1985).

[4] D. B. Kaplan and H. Georgi, Phys. Lett. **B136**, 183 (1984).

[5] C. Csaki, M. Graesser, L. Randall and J. Terning, Phys. Rev. D **62**, 045015 (2000) [arXiv:hep-ph/9911406]; G. F. Giudice, R. Rattazzi and J. D. Wells, Nucl. Phys. B **595**, 250 (2001) [arXiv:hep-ph/0002178].

[6] W. D. Goldberger, B. Grinstein and W. Skiba, Phys. Rev. Lett. **100**, 111802 (2008) [arXiv:0708.1463].

[7] D. Alves *et al.*, [arXiv:1105.2838];

[8] J. A. Evans and M. A. Luty, Phys. Rev. Lett. **103**, 101801 (2009).

[9] S. Chang, J. A. Evans, and M. A. Luty, simplified model "Multiple Weak Bosons from Strong Spin-0 Resonances," `http://lhcnewphysics.org/leptons`.

[10] B. W. Lee, C. Quigg and H. B. Thacker, Phys. Rev. **D16**, 1519 (1977); M. S. Chanowitz and M. K. Gaillard, Nucl. Phys. **B261**, 379 (1985).

[11] J. Bagger *et al.*, Phys. Rev. **D52**, 3878 (1995); J. M. Butterworth, B. E. Cox and J. R. Forshaw, Phys. Rev. **D65**, 096014 (2002);

[12] S. Abdullin, H. Baer, C. Kao, N. Stepanov, and X. Tata, Phys. Rev. D **54**, 6728 (1996).

[13] S. Chang, J. Evans and M. Luty, Phys. Rev. **D84**, 095030 (2011).

[14] J. Evans *et al* arXiv:1201.3691 (2012).

[15] Charged higgs

[16] T. Aaltonen et al.(CDF Collaboration), Phys. Rev. D **71**, 032001 (2005).

[17] C. S. Hill, Nucl. Instrum. Methods A **530**, 1 (2004).

[18] T. Aaltonen et al.(CDF Collaboration), Phys. Rev. Lett. **97**, 082004 (2006); T. Aaltonen et al.(CDF Collaboration), Phys. Rev. Lett. **94**, 091803 (2005).

[19] CDF uses a cylindrical coordinate system with the z axis along the proton beam axis. For a particle or a jet, pseudorapidity is $\eta \equiv -\ln(\tan(\theta/2))$, where θ is the polar angle relative to the proton beam direction, and ϕ is the azimuthal angle while transverse momentum $p_T = |p|\,\sin\theta$,

and the transverse energy $E_T = E\ \sin\theta$.

[20] T. Aaltonen et al.(CDF Collaboration), Phys. Rev. D **45**, 001448 (1992).

[21] A. Bhatti *et al.*, Nucl. Instrum. Methods A **566**, 375 (2006).

[22] Missing transverse momentum, $\not{E}_T$, is defined as the magnitude of the vector $-\sum_i E_T^i \vec{n}_i$ where E_T^i are the magnitudes of transverse energy contained in each calorimeter tower i, and $\vec{n}_i$ is the unit vector from the interaction vertex to the tower cetroid in the transverse (x, y) plane.

[23] T. Aaltonen et al.(CDF Collaboration), Phys. Rev. D **74**, 072006 (2006).

[24] J. Alwall *et al.* J. High Energy Phys. **09** (2007) 028.

[25] T. Sjostrand *et al.*, Comput. Phys. Commun. **238**, 135 (2001), version 6.422.

[26] E. Gerchtein and M. Paulini, arXiv:physics/0306031 (2003).

[27] Electroweak Group (CDF and D0 Collaborations), arXiv:1107.5255 (2011). We use a top-quark mass of 172.5 GeV/c^2 which is compatible with the current Tevatron combination of 173.2$\pm$0.9 GeV/c^2.

[28] U. Langenfeld *et al.*, Phys. Rev. D **80**, 054009 (2009).

[29] S. Frixione, P. Nason, and B. Webber, J. High Energy Phys. **08** (2003) 007.

[30] M. Mangano *et al.*, J. High Energy Phys. **07** (2003) 001.

[31] J. Campbell and R. Ellis, Phys. Rev. D **60**, 113006 (1999).

[32] B. W. Harris *et al.*, Phys. Rev. D **66**, 054024 (2002).

[33] T. Aaltonen et al.(CDF Collaboration), Phys. Rev. D. **73**, 32003 (2006).

[34] A. Read, Nucl. Instrum. Methods A **425**, 357 (1999).

[35] A. Read, J. Phys. G: Nucl. Part. Phys. **28**, 2693 (2002); T. Junk, Nucl. Instrum. Methods A **434**, 425 (1999).